JJ

GSI

GSI-96-04
Report
NOVEMBER 1996
ISSN 0171-4546

STRIPPING OF FAST H^- AND H_2^+ IONS IN FOILS

E.A. Andreev, D. Böhne, V.L. Bychkov, V.P. Shevelko

Gesellschaft für Schwerionenforschung mbH
Planckstraße 1 • D-64291 Darmstadt • Germany
Postfach 11 05 52 • D-64220 Darmstadt • Germany

STRIPPING OF FAST H^- AND H_2^+ IONS IN FOILS

E.A. Andreev[1], D. Böhne[2], V.L. Bychkov[3] and V.P. Shevelko[2*]

[1] N.N. Semenov Institute of Chemical Physics, Russian Academy of Sciences, Kosygina 4, 117977 Moscow, Russia,

[2] GSI, D-64220 Darmstadt, Germany,

[3] Institute for High Temperature Physics, Russian Academy of Sciences, 127412 Moscow, Russia,

[*] *Permanent address*: P.N.Lebedev Physics Institute, Russian Academy of Sciences, Leninsky prospect 53, 117924 Moscow, Russia.

CONTENTS

1. Introduction

2. Atomic Processes in Ion-Foil Low-Energy Collisions (E = 1-30 MeV/u)
2.1 Collisions of H^0 Atoms and H^- Ions With Foils
2.2 Transmission of H_2^+ Ions through Thin Foils

3. Relativistic Energy Range (E = 800 MeV/u - 1.5 GeV/u)
3.1 General Features
3.2 The use of Relativistic H^- and H_2^+ Ion Beams for non-Liuovillian Injection
3.3 Creation of Neutral Hydrogen
3.4 Dissociative Lifetimes of Electronically Excited H_2^+ Molecular States
3.5 Electric-Field Stripping of H^0, H^- and H_2^+

4. Conclusion

1 Introduction

Interaction of fast hydrogenic species H^+, H^0, H^-, H_2^+ and H_3^+ with foils is of great interest from experimenter's viewpoint. Fast (even relativistic) beams of protons H^+ with energy E = 800 - 1300 MeV/u are required to produce intensive neutron fluxes using operating 800 keV/u or planning 1.3 GeV/u regimes [1, 2, 3]. According to the Liouville's Theorem (see, e.g., [4]) applied for acceleration problems, the phase-space acceptance area of an accelerator ring can only be filled once, limiting in the classical multi-turn injection scheme the number of turns of the ratio of ring acceptance over linac beam emmitance. The Liouville's Theorem can be circumvented by a charge changing of passing incident beam through a thin foil applied, hence converting H^-, H_2^+, H_3^+ into the H^+ charge state for subsequent acceleration. The main problem arising in stripping of hydrogenic species in foils is creation of significant fraction of neutral hydrogen (about 5 - 10%) which can be ionized by external magnetic (electric) field in the late stage inside the bending magnet. The protons, formed by field ionization of these "late" atoms, can spoil the original proton beam and produce unexeptable hard radiation after hitting the walls.

Recent development of intense H^- ion sources made it possible to consider the H^- injection as the preferred scheme for most high-intensity proton machines. However, the use of H_2^+ ions as initial beam, can be alternative to H^- case because the former is more stable under stripping by external electric fields and it has a higher production rate in the ion source compared to H^- ions.

Besides acceleration problems mentioned, fast ion-foil collisions constitute a unique possibility for studying atomic collisions processes in solids such as foil-induced dissociation of molecular ions, creation of neutral hydrogen atoms, correlation between target electrons and projectiles, Coulomb repulsion of the nuclei in the foil and other effects. We note, that the majority of these processes are still poorly understood from both experimental and theoretical points of view.

Experimental investigations of ion-foil collisions started in early 1970s, cover two main energy ranges: low energies, E = 1 - 30 MeV/u, and relativistic energy range E = 800 - 1300 MeV/u. To our knowledge, there is no publications on measurements having been performed in the middle-energy range E = 30 - 800 MeV/u.

Our aim in this work is to consider two main aspects:

a) atomic collision processes occuring when the hydrogenic species passing through thin foils and, especially, a production of emerging fraction of excited neutral hydrogen atoms $H^*(n)$;

b) a possibility of using H^- and H_2^+ ion beams for producing the dense fast proton beams.

Problems a) and b) are closely related each other because the main losses in H^- and H_2^+ beams passing through foils are caused by creation of neutral hydrogen atoms in the

ground or excited states.

2 Atomic Processes in Ion-Foil Low-Energy Collisions (E = 1 - 30 MeV/u)

Collisions of ions with foils in this energy range are investigated in many papers experimentally [5, 6, 7, 8, 9, 10, 11, 12] and theoretically [12, 13, 14, 15, 16, 17]. Here, we consider the atomic processes arising in collisions of neutral H^0 atoms and H_2^+ and H^- ions with thin, 1 - 100 $\mu g/cm^2$, carbon foils (thickness of 1 $\mu g/cm^2$ corresponds to approximately 50 Å).

2.1 Collisions of H^0 Atoms and H^- Ions with Foils

To understand the physics of ion-foil collisions, we start with the simple case of the incident neutral hydrogen beam. Typical experimental scheme employed to produce a *neutral* incident beam and to measure the *neutral* fraction $\Phi(H^0)$ in the transmitted beam is shown in Fig. 1 for a 2 MeV H^0 beam (corresponding velocity $v \approx 10$ a.u., 1 a.u. $= 2.28 \times 10^8$ cm/s) colliding with a carbon foil of a thickness $x = 2$ - 10 $\mu g/cm^2$.

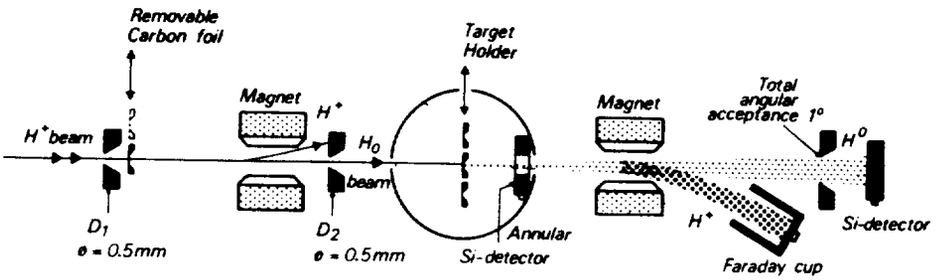

Figure 1: Experimental arrangment for measuring a fraction $\Phi(H^0)$ of neutral atoms with an incident neutral beam. From [8]

In this range of velocities and thicknesses, a change of projectile velocity inside the target is negligible and the *dwell time* t_D, i.e. a time spent by progectile inside a foil, is given by a simple relation $t_D = x/v$ and lies in the 1 - 40 fs range. Although almost all hydrogen atoms are converted into proton beam (96-98%), these is a small fraction of neutral atoms ($\sim$ 5%) still emerging the foil.

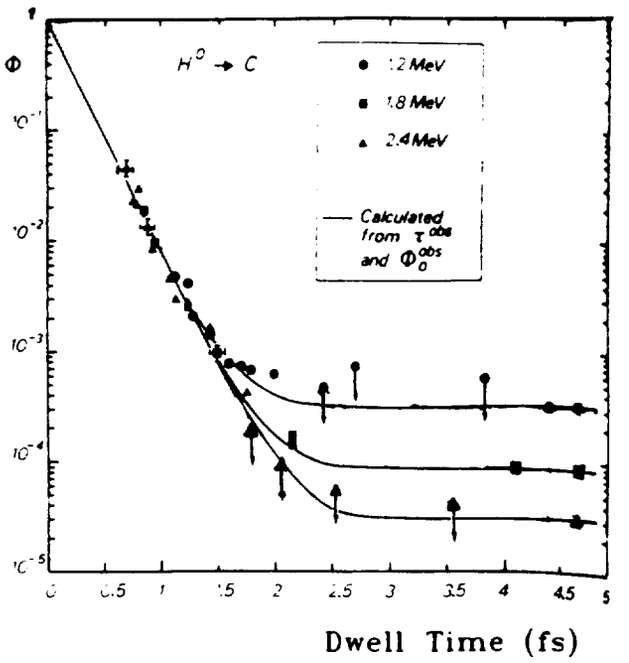

Figure 2: Measured fraction $\Phi(H^0)$ of neutral atoms emerging from the carbon foil as a function of the projectile dwell time. From [8]

A measured emerging neutral fraction $\Phi(H^0)$ as a function of t_D is displayed in Fig. 2. There are two different regimes seen in the Figure: the *equilibrium* regime at $t_D > 2.5$ fs where the fraction Φ_0 is independent on t_D but depends on the projectile velocity v, and $non - equilibrium$ regime, $t_D < 2.5$ fs, with a fraction of created neutral atoms exponentially increasing ($\sim exp(-t_D/\tau)$) with t_D decreasing, where τ is experimental time-dimension constant independent on v: $\tau(H^0) = (2.12 \pm 0.18) \times 10^{-16}$ s. The quantity τ can be prescribed to the *distruction* or *electron – loss* cross section σ_l of hydrogen atom in a solid:

$$\tau = (Nv\sigma_l)^{-1}, \tag{1}$$

where N is the foil density. The fact that τ does not depend on velocity means that in the energy range considered, the cross section $\sigma_l \sim v^{-1}$, as predicted by Bohr [19] for light ions in a solid matter.

According to experimental data, the incident H^0 atom looses its electron after passing first few atomic layers in the foil, hence a neutral H atom is formed via a capture of a foil-electron by a proton with a certain cross section σ_c. The standard calculations show that the fraction of protons and neutral hydrogen at the foil thickness x can be written, respectively:

$$\Phi(H^+) = \frac{\sigma_l}{\sigma_l + \sigma_c} + \left(1 - \frac{\sigma_l}{\sigma_l + \sigma_c}\right) e^{-(\sigma_l + \sigma_c)Nx}, \tag{2}$$

$$\Phi(\mathrm{H}^0) = \frac{\sigma_c}{\sigma_l + \sigma_c} + \left(1 - \frac{\sigma_c}{\sigma_l + \sigma_c}\right) e^{-(\sigma_l + \sigma_c)Nx}, \quad (3)$$

In the equilibrium regime, the neutral fraction is a constant value defined by the ratio of the capture and loss cross sections:

$$\Phi_0(\mathrm{H}^0) = \frac{\sigma_c}{\sigma_c + \sigma_l} \approx \sigma_c/\sigma_l, \text{ and} \quad (4)$$

$$\Phi_0(\mathrm{H}^+) = \frac{\sigma_l}{\sigma_c + \sigma_l} \approx 1 - \sigma_c/\sigma_l, \quad (5)$$

since in the energy range considered $\sigma_c \ll \sigma_l$. From experimental values of τ and $\Phi_0(\mathrm{H}^0)$ and eqs. (1, 5) it is possible to estimate cross sections σ_c and σ_l; they are in agreement with the cross sections meausured for hydrogen atoms in gases [18] (see Table 1).

Table 1: Electron-loss (H + C) and capture (H^+ + C) cross sections as obtained from experiments in foils [8] and gases [18]

Proton energy MeV/u	σ_l^{foil} (10^{-17} cm^2)	σ_l^{gas} (10^{-17} cm^2)	σ_c^{foil} (10^{-21} cm^2)	σ_c^{gas} (10^{-21} cm^2)
1.2	3.75 ± 0.3	5.0	11.7 ± 2.2	13.0
1.8	3.1 ± 0.25	4.1	2.7 ± 0.5	3.2
2.4	2.7 ± 0.25	3.1	0.8 ± 0.15	1.2

We note that these data are well described by the formulas by *Brandt* and *Sizmann* [14] for protons moving with the velocity v inside a solid target of atomic number Z_T:

$$\sigma_c = \frac{2^{18} Z_T^5}{5v^6} (v^2 + 2^6 40^{-1/3} Z_T^{14/9})^{-3} \pi a_0^2 \quad (6)$$

$$\sigma_l = \frac{Z_T^{2/3}}{Z_T^{2/3} + v} \left(\frac{4 Z_T^{1/3} (Z_T + 1)}{4 Z_T^{1/3} (Z_T + 1) + v} \right) \pi a_0^2 \quad (7)$$

where a_0 is the Bohr radius and a velocity v is in atomic units.

In gas targets, the loss and capture cross sections are quite easy to measure and calculate; at $v \approx 10$ a.u., they behave as $\sigma_l \sim v^{-1}$ and $\sigma_c \sim v^{-6}$. We note that in usual case of binary ion-atom collisions, dependence of σ_l and σ_c on v is much more stronger: $\sigma_l \sim (lnv)/v^2$ and $\sigma_c \sim v^{-12}$ (see, e.g., [20]).

It is well known that in the velocity range $v \sim 10$ a.u., the electron capture occurs mainly to the states H(nl) with the principal quantum numbers $n = 1$ and 2; for higher

Table 2: Relative initial population of foil-excited hydrogen states created by incident H atoms and H_2^+ molecules (from [22])

Population ratio	Statistical $(2l+1)/n^3$	Experimental Protons	results Molecules	Present paper (protons)
N^0_{2s}/N^0_{1s}	0.125	-	-	0.125
N^0_{2p}/N^0_{2s}	3	-	-	0.74
N^0_{3p}/N^0_{3s}	3	0.608 ± 0.033	1.08 ± 0.11	0.73
N^0_{3d}/N^0_{3s}	5	0.422 ± 0.022	1.29 ± 0.11	0.30
N^0_{3p}/N^0_{2p}	0.296	0.211 ± 0.007	1.234 ± 0.016	0.296

states, $n \geq 3$, the cross section σ_c falls off according to a n^{-3} law. In the proton-atom electron capture, the states H(nl) with $l = 0$ and 1 are mostly populated (see Table 2).

The last row of the table reflects the n^{-3} dependence. In the present paper, a population of the nl-state in hydrogen was estimated using theoretical results [21] for charge-exchange cross sections, gives the following nl-dependence

$$\Phi_0(nl) \sim \frac{2l+1}{n^3} exp(-1.4l) \tag{8}$$

and also presented in Table 2 in the last column.This law was also confirmed by experiments for fast ions penetrating through carbon foils (see, e.g., [22, 23, 24, 25]). The total fraction of neutral hydrogen in collisions of 1 MeV H-atoms with 1 - 8 μg/cm^2 thickness carbon is about 8×10^{-4} as shown in Fig. 3.

In ion-foil experiments, a creation of a neutral atom is related with different processes taking place inside the foil and at its surface. According to *Brandt* and *Sizmann* [14], in proton-foil collisions, two main processes are responsible for formation of a neutral hydrogen. The first one occurs in the bulk and is a collision in which a target electron gains correlation in speed and direction with the moving proton. The second one takes place at the exit surface and is an electron capture into a bound state provided the correlation has not been lost. Therefore, collisions of ions with foils are more complicated compared to binary ion-atom collisions. However, in practice, the quantitative description of the ion-foil collisions, a hydrogenic scaling for the effective cross sections are used, hence the processes in solids are treated similar to those in gases.

Collisions of H^- ions, having two bound electrons, reveal similar behavior as H^0 incident atoms. For example, the measurements with carbon foils at MeV regime show similar transmitted fraction and neutral fraction as for H^0 projectiles (Fig. 3). Using this experimental fact, the authors in [9] make more general assumption that in the energy regime

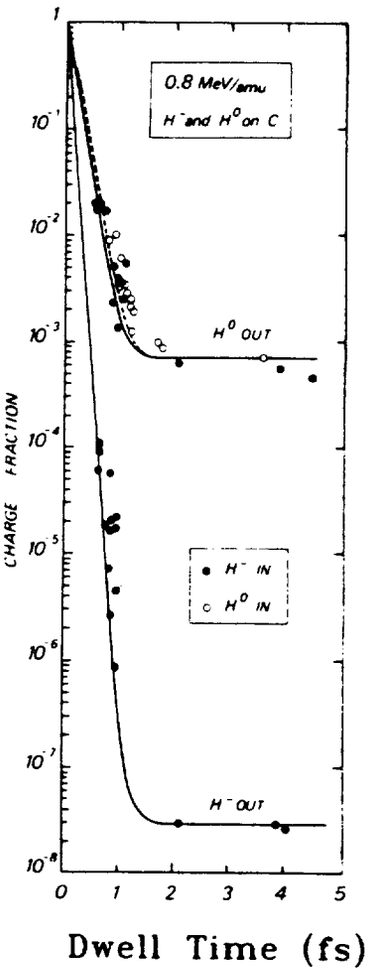

Figure 3: Transmitted fraction of incident H^0 and H^- and the H^0 fraction from incident H^- ions. From [9]

considered, the emerging fractions arising in collisions of light ions H^0, H^-, He^0, He^+, H_2^+, H_3^+ can be described by hydrogenic scaling within the Born approximation. In this respect, the projectile is represented with an effective charge Z_{eff} corresponding to the hydrogenic wavefunction and energy. The Z_{eff} values of 1.0, 0.7, 1.7, 2.0, 1.1 and 1.5 are used for loss and capture cross sections. In other words, inside the solid these loosly bound systems can be described by a free ion approach. The difference is that processes in solids have higher collision frequency due to a higher density of target atoms in solids. However, we will see in Section 2.2, that the effective charge Z_{eff} of the molecular ion depends, in general, on the internuclear distance R.

2.2 Transmission of H_2^+ Ions through Thin Foils

The H_2^+ ions have one bound electron but two protons that makes the problem much more complicated as compared to the incident H^0 or H^- simple projectiles. Collisions of hydrogenic molecules with foils are characterized by the following features [23]:

1. Penetration of the projectile into the foil before loss of original electrons;

2. Coulomb repulsion of protons, created in the foil by stripping;

3. Polarization of the target electron plasma by protons (wake forces) which affects the repulsive motion of protons.

Atomic processes arising in collisions of H_2^+ ions with thin carbon foils, seem to be well understood experimentally [8, 9, 17, 26] and theoretically [12, 13, 17, 27]. These investigations include transmission yields, stopping and scattering-angle distributions of molecular ions traversing carbon foils in a wide thickness range (x = 1 - 15 μg/cm^2) and incident projectile energies (E = 0.4 - 1.2 MeV/u).

Fast ($\sim$ MeV) light ions colliding with a foil loose their binding electrons within the first few atomic layers of the target because of the characteristically large electron-loss cross sections ($\sim 10^{-16}$ cm^2). As was shown experimentally, lifetimes of incoming projectiles H^0, H_2^+, H^- and H_3^+ depend only on number of bound electrons and constitute, respectively, [26]: $\tau(H^0) = (2.1 \pm 0.1) \times 10^{-16}$ s, $\tau(H_2^+) = (1.9 \pm 0.2) \times 10^{-16}$ s, $\tau(H^-) \sim \tau(H_3^+)$ = and $(1.18 \pm 0.13) \times 10^{-16}$ s.

One of the important subject arising in investigations of ion-foil collisions is a transmission of fast ions through thin foils and creation of neutral hydrogen. A measured [17] transmission factor for H_2^+ in carbon foils for incident H_2^+ ions as a function of a dwell time t_D is displayed in Fig. 4.

At $t_D < 1$ fs, a transmission yield of H_2^+ is exponentially small $\sim \exp(-\, t_D/\tau)$ with τ = 0.17 fs and is independent on the projectile velocity. This exponential fall can be related

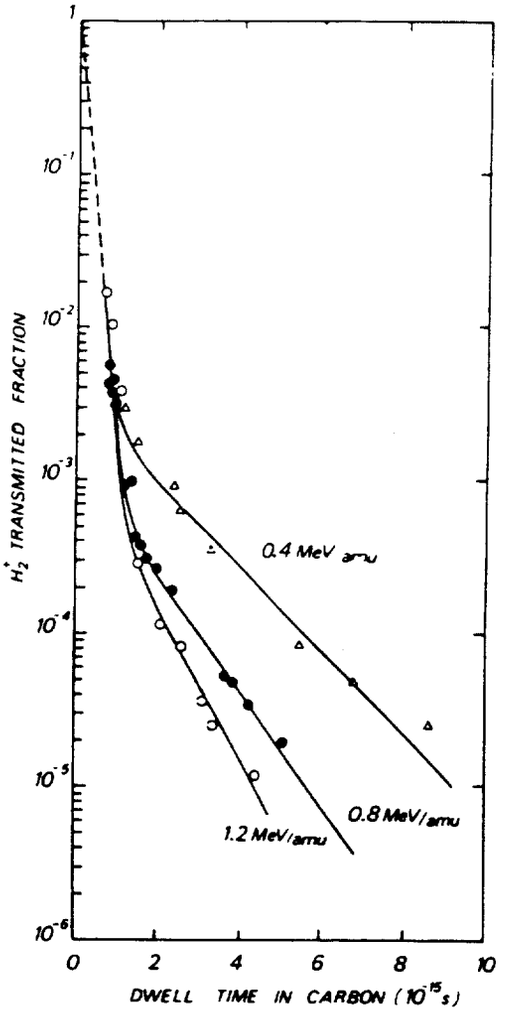

Figure 4: Transmitted fraction of incident H_2^+ from incident H_2^+ ions. From [17]

to the electron loss in a solid state with the corresponding electron-loss cross section given by eq 1. This region is characterized by the survival of the incident projectiles that come through the foil with their own (*original*) electrons. A previous measurement of H^0 yield with incident H_2^+ [8] also shows the exponential decay with increasing t_D, that correlated with H_2^+ transmission yield, and can be viewed to originate from the *dissociation* of the incident H_2^+ ions being mostly in the ground $1s\sigma_g$ state:

$$H_2^+ \rightarrow H^+ + H(nl). \tag{9}$$

The region $t_D > 1$ fs is characterised by a strong dependence on the projectile velocity v when the incident ion molecules pass through a foil with other (*reconstituted*) electrons captured from the *target*. After loosing its electron, two rest protons exhibit the Coulomb repulsion in the foil with characteristic time for the Coulomb explosion (a few fs) generally compared to the dwell time. The capture occurs at the exit of the foil and can proceed into molecular orbits either bonding or dissociative depending on the internuclear distance R at the exit and relative internal kinetic energy E_k of diproton. Excited molecular states dissociate into a proton and a hydrogen atom in the ground or excited states (see Fig. 5; for example:

$$H_2^+(3s\sigma_g) \rightarrow H^+ + H^0(3s), \tag{10}$$
$$H_2^+(2p\pi_u) \rightarrow H^+ + H^0(2p), \tag{11}$$
$$H_2^+(2p\sigma_u) \rightarrow H^+ + H^0(1s), \tag{12}$$
$$H_2^+(1s\sigma_g) \rightarrow H^+ + H^0(1s) \tag{13}$$

The only one reaction leading to creation of the ground state $H^0(1s)$ from excited molecular state is reaction (12). The reaction (13) takes place if $E_k + U(1s\sigma_g) > 0$. If $E_k + U(1s\sigma_g) \leq 0$, it means that the original electron of the incident molecule is not lost after passing through the foil.

The question arises about how these excited molecular states are populated.It was seen that the probability of creation of the bound (or not bound) molecular state strongly depends on the internuclear distance R and relative energy of two protons $\mu(dR/dt)^2/2$ where μ is the reduced mass of two protons (Fig.6).The initial separations R_0 in H_2^+ and H_3^+ ions are 1.3 and 1.1 Å, respectively.

At present, there is no satisfactory theory of electron capture into molecular-orbital states. However, a good estimation of the molecular capture cross section is given by the hydrogenic scaling relation suggested in [17]:

$$\sigma_c^{mol}(v) = Z_{mol}^5(R)\sigma_c^H(v), \tag{14}$$

where $\sigma_c^H(v)$ is the capture cross section for atomic hydrogen at the same velocity v and $Z_{mol}(R)$ is the effective charge of the two nuclei for the capture into molecular states. For

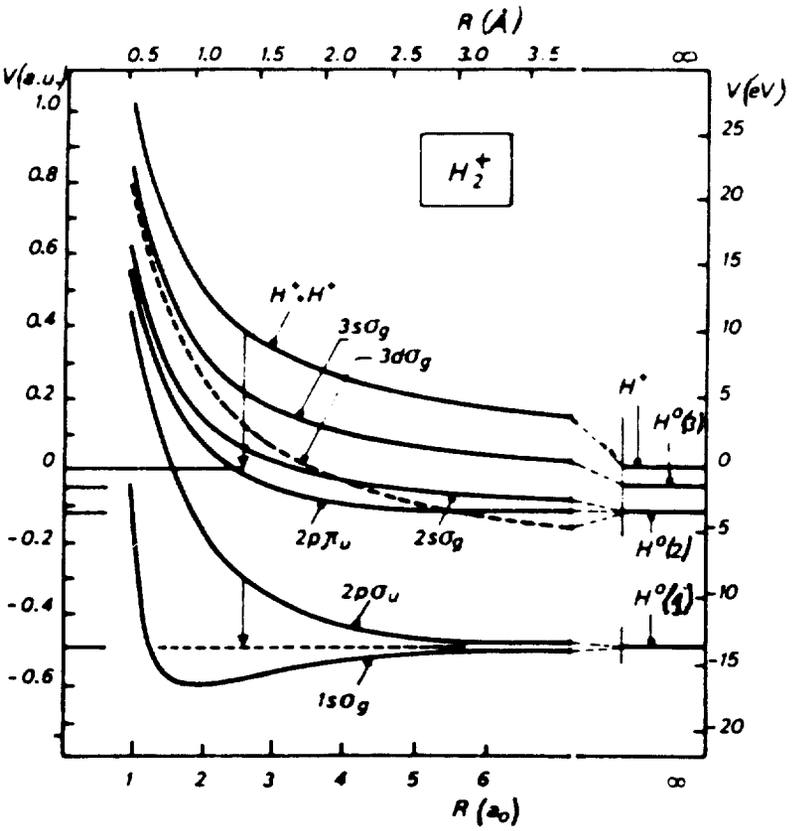

Figure 5: Potential energy curves of H_2^+. From [8]

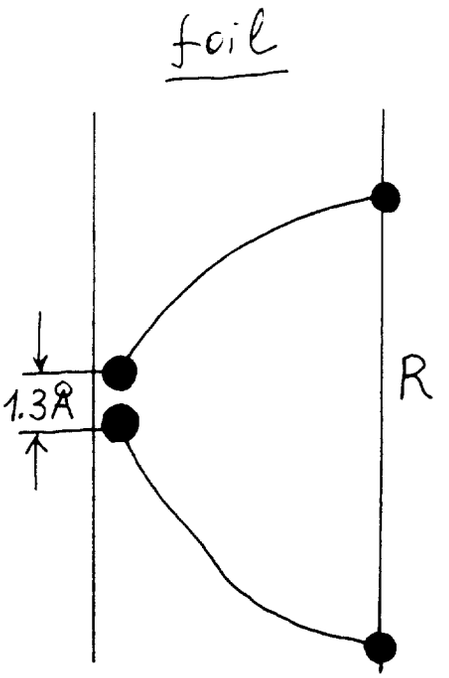

Figure 6: Coulomb repulsion of two formed protons after stripping H_2^+ ions in the foil

$1s$ g-state it reads [28]:

$$Z_g(R) = 1 + exp(-0.76)R, \tag{15}$$

with R in atomic units.

The scaling (14) follows from experimental results, for example, as shown by experiments [22], the population of H(nl) levels of high angular momentum is 2 - 3 times larger in the case of H_2^+ molecules as compared to protons (Table 2) because of influence of two main processes:

1. Dissociation carrying out original (molecular) electrons,

2. Electron capture of the target electrons into molecular excited states followed by dissocoation into protons and H*(nl) atoms.

There are a few experimental meausrements [29, 30, 31] indicating that the n^{-3} law is valid only for low principal numbers of resulting hydrogen atoms, $n < 5$; for higher $10 < n < 14$ these experimental data follow n^{-p}-law with $p = 8.0 \pm 1.0$.

A probability of having a bound molecule at a given inter-proton distance R is then given by

$$P_b(R) = \frac{\sigma_c^{mol}}{(\sigma_c^{mol} + \sigma_l^H)}, \text{if } E_k + U(R) \leq 0,\ E_k = \mu V^2/2, \tag{16}$$

$$P_b(R) = 0, \text{ otherwise}, \tag{17}$$

where μ is the reduced mass of dicluster and V is their relative velocity in the foil; σ_l^H is the loss-cross section of hydrogen from $1s$-state which is found (experimentally) being the same for H and H_2^+ at the same velocity. The fraction of neutral hydrogen Φ_0 H^0 is given, as before, by eq.(4). The mean value of the probability $P_b(R)$ is obtained by averaging (16) over R-distribution (see [27]). Due to the similarity of the velocity dependence of the molecular and atomic cross sections for electron loss and capture, the following ratio is plotted for transmitted H_2^+ fraction through the carbon foil

$$\Phi(H_2^+)/\Phi(H^0) = \Phi(H_2^+)/\frac{\sigma_c^H}{\sigma_c^H + \sigma_l^H}, \tag{18}$$

which is nearly universal curve as a function of the dwell time t_D independent on the incident ion energy.

At present, the sophisticated theories take the following effects into account to calculate fractions of H_2^+ and H(nl) within accuracy of a factor of 2:

1. Initial distribution of H_2^+ over vibrational states,

2. Coulomb repulstion of protons inside the foil.

3. Electron capture into excited molecular states.

4. Wake (polarization) effects of the target electrons by the cluster.

5. Scattering of protons by target electrons.

Fig. 7 shows a universal dependence of the ratio of emerging fractions H_2^+ and H(nl) particles as a function of the dwell time corresponding to a wide energy range (E = 0.4 - 1.2 MeV/u) of the incident H_2^+ ions and dwell time (t_D = 0 - 30 fs).

In the end of this Section , the following conclusions can be made:

1. Incident ions can penetrate a foil being unchanged with their own (original) electrons.

2. Fraction of neutral H(n) can be quite large (about 10^{-3})and is caused by electron capture from the exit surface of the foil.

3. The processes of transmitting and emerging of the particles are described in terms of the ion-gas interactions.

4. Yield of neutrals H(n) is independent on the foil thickness.

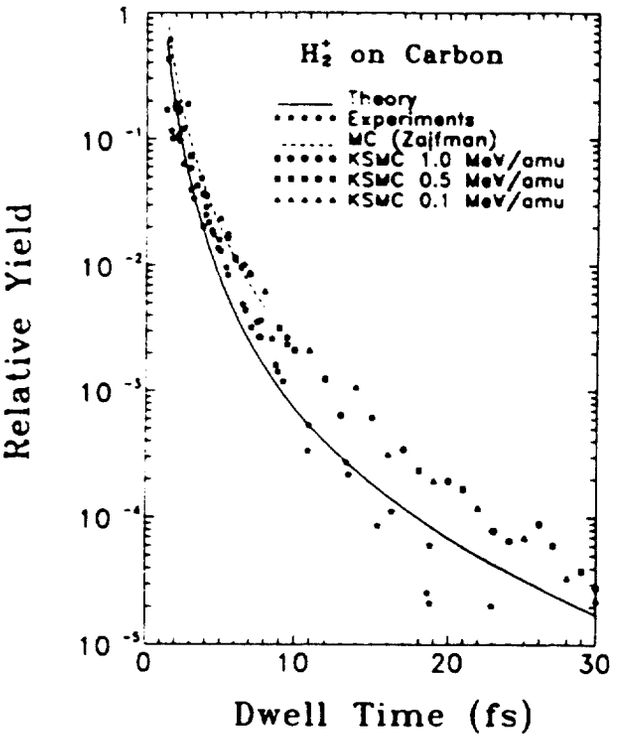

Figure 7: Relative transmission yield of H_2^+ ions in C-foil. From [27]

5. In the case of incident molecular ions, the Coulomb repulsion of the nuclei in the bulk plays a key role at low-energy regime.

3 Relativistic Energy Range (E = 800 MeV/u - 1.5 GeV/u)

3.1 General Features

Experimental and theoretical data on collisions of relativistic ions with foils are very scarce (see, e.g., [32, 33, 39, 38]) and are known mostly for H^- ions colliding with 15 - 300 $\mu g/cm^2$ carbon and Al_2O_3 foils. Although the size of H^- ion is about 4 Å and that for a solid carbon about 2 Å, quite a finite fraction of H^- ions is survived after passing through a foil.

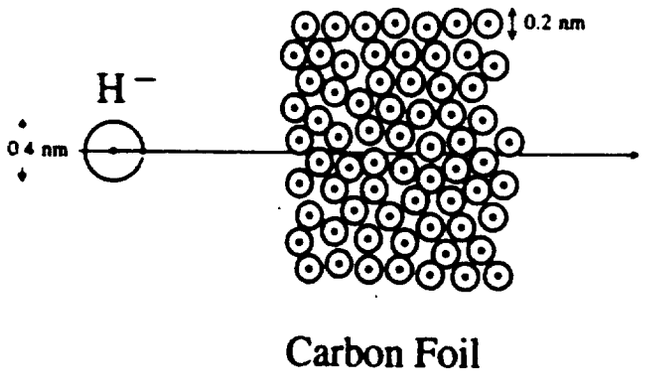

Figure 8: The relative sizes of the outer electron orbits for the H^- ion and the carbon atoms from the foil. From [32]

Experimental data have shown a significant difference of relativistic ion-foil collisions as compared to those at low-energy energies (Sect. 2.1). Briefly, they can be formulated as follows:

1. Interaction time of relativistic ions with foil is very small: $t_D < 0.5$ fs.
2. Electron capture cross sections are negligible (v^{-6}) at these energies, hence another mechanisms take place. For creation of H(nl) the most probable one is a stepwise excitation or simultaneous ioniation-excitation processes caused by chaotic collisions with the target atoms.
3. At these energies, highest orbital l-states are mostly populated (not low as in gases)

with the following law for the principal quantum numbers: $\Phi(nl) \sim n^p$ with $1.3 < p < 3.5$.
4. Excited states are created inside the foil, but not at the exit, therefore the bulk effects dominate the surface effects.
5. The approximation of ion-gas interaction, which is more or less acceptable at low energies, is not valid any more. More probably, this interaction constitutes a chaotic process.

At present, there are three main approaches used for description of high-energy ion-foil collisions: a quantum chaos when an electron in the hydrogen atom exhibits stochastic collisions with the target atom, so-called microwave-field approximation [41], a high-frequency laser-pulse model [42, 43] and a calssical stochastic dynamics treatment [33, 40]. The latter employs a stochastic version of Newton's equation of motion, i.e., a miscroscopic Langevin equation:

$$d\mathbf{v}/dt = -\nabla V_p + \mathbf{F}_r(t), \tag{19}$$

where V_p is a screened potential of a proton and $F(t)$ is the random fluctuating force described by a sequence of sudden, impulsive momentum transfers ("kicks"),

$$\mathbf{F}(t) = \sum_{a=1,2} \sum_i \Delta \mathbf{P}_i^a \delta(t - t_i^a), \tag{20}$$

where $\Delta \mathbf{P}_i^a$ is the stochastic momentum transfer to the electron per collision at time t_i^a being a random sequence.

This model seems to be providing some insights into the nature of relativistic H^--foil collisions. Fig. 9 shows a quantitative agreement of calculated fragment fractions with absolute experimental data in the case of relativistic H^--foil collisions; same calculations for n-distributions of resulting hydrogen atoms on n are shown in Fig. 10.

3.2 The use of Relativistic H^- and H_2^+ Ion Beams for Non-Liouvillian Injection

In a classical high-energy proton accelerator, the beam, generated by a H^+ ion source, is preaccelerated by a rf linac and then injected into the synchrotron ring. The revolution time of one turn is only a few μ-seconds, hence the number of delivered particles is low. One aims at injecting more turns, usually about 30 ± 10 turns. This is called the *multiturn injection.* It is problematic in the following sense: the phase space acceptance of the ring, which actually can be made much higher than the emittance of the linac beam, can only be filled once due to *Liouville's Theorem.* This holds true also for any subsection of the phase space. The injected turn is magnetically moved away sequentially in the ring vacuum chamber to make room for the next injected turn. This requires a thin electrostatic septum inside the ring, separating the injection orbit from the already circulating beam.

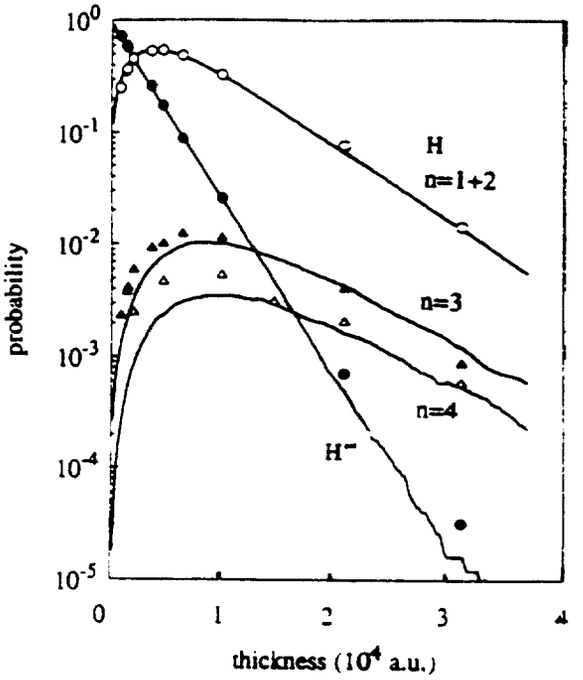

Figure 9: Caculated yields of H^- and H(n) with n = 1 - 4 (solid curves) incomparison with experiment (symbols) at energy E = 800 Mev. From [33]

This method involves unavoidable beam losses of 20 $\pm$ 10 % due to the shadowing of the septum.

The demand for higher and higher beam intensities arouse in the last three decades since the elementary partice research concentrated more and more on rare collision events. The intensity increase became a problem of beam losses and hence an activation of the synchrotron. The losses, unfortunately, are not localized, rather than distributed around the ring due to scattering effects at the septum. In the very early machines this situation was not a concern, because this effect occured at the internal production target anyway. The only sheme for a nearly loss-free injection proposed and experienced until now is the circumvention of Liouville's Theorem by accelerating H^- ions and injecting them accross a thin stripping foil in a corner of the vacuum chamber, thus converting the H^- beam into a circulating high density H^+ beam with a theoretically unlimited number of turns.

Space charge constraints limited the intensity of the circulating beam: around 100 turns are usual and 1000 turns are possible. Beam losses are around 2% by conversion of H^- into H^0 in the foil, but these neutral particles leave the ring straight ahead from the foil and are dumped locally. The challenge of increasing the turn number allowed for modest source currents. The present state of source development is typically 35 mA for low duty cycle operation. A further concern with the H^- ions is its subceptability to stripping-off the very loosely bound electron. This is not a problem considering residual gas collisions in the linac. It is a problem, increasing with energy, considering Lorenz stripping in the

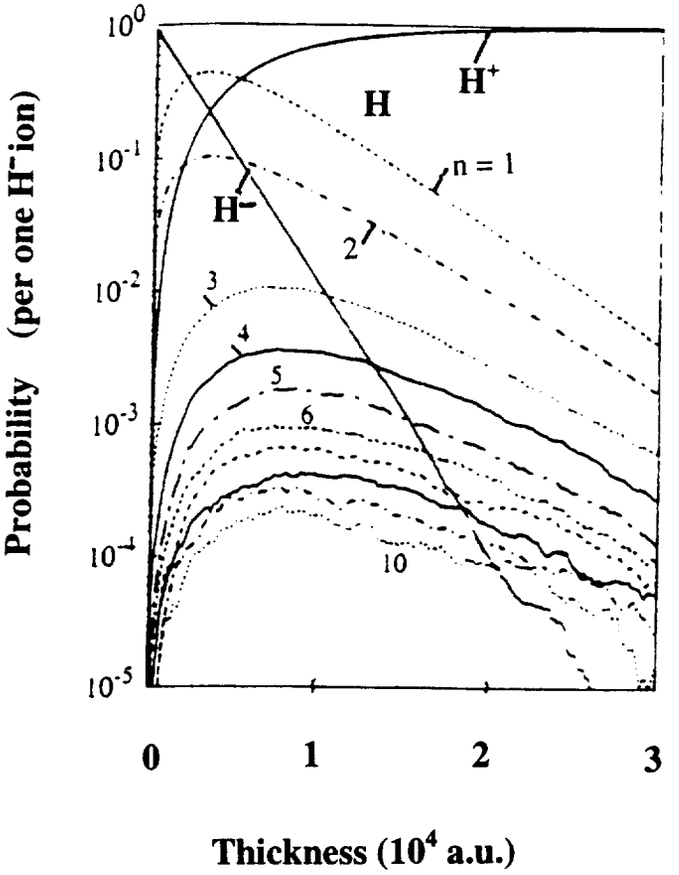

Figure 10: Same as in Fig. 9 for n = 1 - 10 (theory). From [33]

many magnetic elements. This effect can be reduced to tolerable values by reducing the magnetic field strength. The consequently longer dimensions of the magnetic elements results in difficult design constraints.

This paper reconsiders the atomic physics issues of using H_2^+ ions instead of H^- ions for the non-Liouvillian injection into a high energy accumulator ring, which is instrumental in the context of future pulsed spallation sources, presently under study in Europe and the USA. The design value of the average beam power involved amounts to 5 MW, which is 30 times higher then record values achieved so far. The outlined increase is a combination of a slight increase of beam energy and a considerable increase in beam intensity in the full energy linac (the accumulator ring does not accelerate). Most notably a further reduction of the beam losses at injection is imperative.

The use of H_2^+ in this context was proposed several times in the past. It was rejected because for the same final energy a H_2^+ linac would have been twice as long as a H^- linac and would require twice the rf power for the ohmic wall losses of the rf accelerating cavities (but not for building up the required beam power!).

This argument has nearly disappeared, since superconducting (SC) cavities are strongly under consideration anyway. SC cavities allow for a considerable increase in the energy gain per unit length, while still demanding zero wall current losses. The expensive rf power entirely goes into the beam power. The possible favourable reduction of the electrical beam current by a factor of two, when doubling the linac voltage, is highly desirable. This reduction of the electrical beam current eases the particle dynamic problems, encountered in the evaluation of space charge effects.

On the technical side a different situation persists for H^- beams: no ion source is available or even is considered for the required 140 mA beam current. It is presently proposed therefore, to combine at the low energy end of the linac two beams from 70 mA H^- sources. Some scepticism is expressed, whether even this value can be attained for high duty factor (6%) sources. In addition, the beam combination, termed *funneling* can impair the transversal beam properties, hence leading to untolerable beam losses in the high energy section of the linac, if the system is not ideally tuned and aligned.

However, the beam transport architecture at injection, the H_2^+ beam now coming from the same side as the curculating H^+ beam, has not been worked out yet.

In reconsidering the H_2^+ case, for which ample of beam intensity can be produced in a single source (nearly same value as in the well experienced H^+ sources), the following questions have to be adressed to the atomic physics side:

a. the fraction of H^0 leaving the foil after stripping the incident H_2^+ beam,

b. susceptibility for Lorentz stripping of H_2^+ compared to H^-,

c. the fraction of H^0 beam in excited states and decaying to H^+ in time intervals short enough that the created H^+ particles still stay in the aperture of the beam pipe. It then would be subject to undesirable oscillations around the central orbit, hence eventually

leading to unacceptable beam losses around the ring,

d. the loss associated with inelastic scattering,

e. the negative momentum tail and emittance increase due to foil scattering.

3.3 Creation of Neutral Hydrogen

The most experimental data on stripping relativisitc H^- ions have been carried out at the Proton Storage Ring at the Los Alamos Meson Physics Facility (LAMPF). The main losses are caused by the ring bending magnets field-ionizating excited-state H^0 atoms not stripped by the foil. These protons can soon collide with the walls of the ring because they are produced at a point where their trajectories are outside the clean acceptance of the ring [45, 46].

The foil thickness is chosen to provide a high stripping efficiency without introducing appreciable scattering and spread of beam momenta. Typically, the strippig efficiency is 96% with 4% remaining mainly as neutral H^0 atoms which have to be removed efficiently from the ring. However, many of H^0 atoms exist in an excited states and may strip to protons in the magnetic fields of the ring, becoming lost before being removed. The question arises on how best to design the injection system to minimise this effect. The lifetimes τ of excited n states of hydrogen atoms are given in Table 3.

Table 3: Lifetimes of excited H*(n) atoms. From [47]

n	τ, s	n	τ, s
2	2.1×10^{-9}	10	1.9×10^{-7}
3	1.0×10^{-8}	15	1.2×10^{-6}
4	3.3×10^{-8}	20	4.6×10^{-6}
5	8.6×10^{-8}		

These lifetimes have to be compared with the time t_0 spent by ions after passing through the foil in the flight pass (before the magnet) with a length L. For 1.334 GeV H^- ions, corresponding to ion velocity $v = 0.9\ c \approx 2.7\times10^{10}$cm/s and $L \approx 2.5$ m, one has $t_0 = L/v \approx 9.2\times10^{-9}$s $\approx 10^{-8}$s. As seen from Table 3, that the neutral $H^*(n)$ atoms with the principal quantum numbers $n \geq 3$ have lifetimes larger than time required to reach the first dipole magnet: $\tau \geq t_0 = 10^{-8}$. In going some distance inside the magnet, these atoms will be stripped and protons arising from $H^*(n), n \geq 3$ will not be deflected as much as protons that were created at the stripping foil and thus will have an angular displacement with respect to the central trajectory of the proton beam (Fig. 11). These losses (also called "first-turn" losses) caused by production of excited H*(n) atoms, constitute about 0.2-0.3%

in the Proton Storage Ring (PSR) at the Los Alamos Meson Physics Facility (LAMPF) (see [1, 32, 33, 38]).

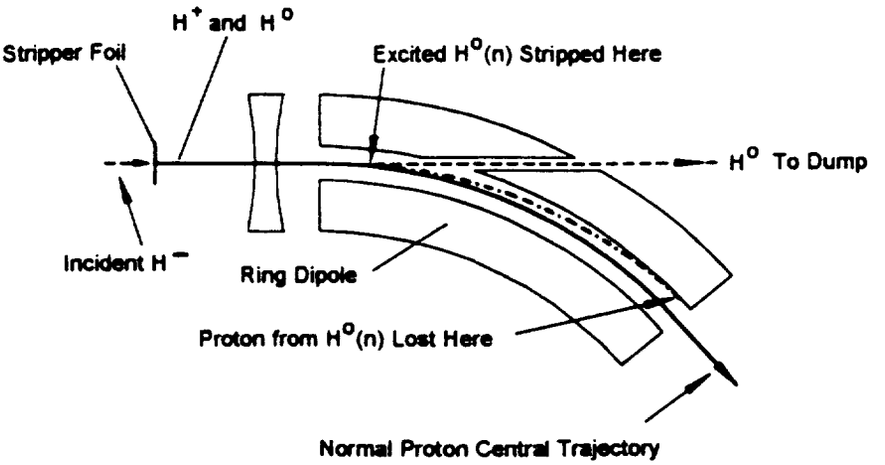

Figure 11: PSR injection region and the origin of the first-turn losses. From [1]

In the case of H^- collisions, the H(nl) atoms can be formed by two main processes: stepwise excitation and simultaneous ionization-excitation caused by collisions with the foil atoms, namely,

$$H^- \rightarrow H(1s) \rightarrow +H^*(nl) + e, \tag{21}$$

$$H^- \rightarrow H^*(nl) + e. \tag{22}$$

With account f0r these processes, the sophisticated calculations [38] of the neutral H fraction show a good agreement with available experimental data. A typical distribution of the resulting particles, H^+, H^- and $H^*(nl)$, for the incident H^- ions at energy $E = 500$ MeV passing through a $200\mu g/cm^2$ foil is given in Table 4. One can see that in this case the fraction of neutral hydrogen is about 5%.

3.4 Dissociative Lifetimes of Electronically Excited H_2^+ Molecular States

To our knowledge, there is no experimental and theoretical data available for processes occuring on foils bombared with relativistic H_2^+ molecular ions. In principal, one can consider two main processes leading to creation of neutral $H^*(n)$ atoms due to interaction of H_2^+ ions with foils: dissociation in the foil with simultaneous excitation of H atoms, and excitation of H_2^+ ions into electronic states followed by dissociation, respectively,

Table 4: Probability per one incident H^- ion of an energy $E = 500$ MeV for creation different fragments after passing a $200\mu g/cm^2$ thickness foil. From [33]

H^+	0.95	H(n=4)	1.5×10^{-3}
H^-	1.0×10^{-4}	H(n=5)	7.0×10^{-4}
H(n=1)	3.5×10^{-2}	H(n=6)	5.0×10^{-4}
H(n=2)	1.2×10^{-2}	H(n=7)	2.5×10^{-4}
H(n=3)	3.0×10^{-3}	H(n=8)	1.7×10^{-4}

$$H_2^+ \rightarrow H^+ + H^*(n) \quad (23)$$

$$H_2^+ \rightarrow (H_2^+)^* \rightarrow H^+ + H^*(n) \quad (24)$$

In process (23), we assume that the fraction of neutral H(nl) atoms will be approximately the same as in H^- case because they are created by stochastic collisions of atomic hydrogen with the target atoms similar to process (21). The processes (24) can also contribute to the neutral fraction production because, at dwell times $t_D \approx 1$ fs the fraction of H_2^+ ions (about 5%, Fig. 4) can come through the foil unchanged but excited into electronic states. (Some decays of excited molecular ions are shown by eqs.(10 - 13)). These states, in turn, can dissociate into protons and hydrogen atoms in the ground or excited states. For the latter processes, one has to know the dissociative lifetimes τ of excited H_2^+ ions in order to compare them with the flight time of protons before they pass through the first magnet ($t_0 \approx 10^{-8}$ s). Corresponding calculations have been performed in [44] using a quasi-classical approach for under-barrier transitions in H_2^+ ions with molecular energy terms approximated by the Morse potential. The calculated values of τ are presented in Table 5 together with energy depth D of the bound molecular state and corresponding equilibrium internuclear distance R_e for the lowest molecular terms.

Calculated lifetimes, $\tau \approx 3 \times 10^{-14}$ s, are found to be very short as compared to the proton flight time before a bending magnet, $t_0 \approx 10^{-8}$ s, which means that the excited H_2^+ ions will decay much earlier before reaching the first magnet. There is no sophisticated calculations of the neutral hydrogen fraction in the case of H_2^+ molecular ions. Using results and conclusions of the present paper, we can only estimate this fraction of about 2 times larger than in the case of H^- ions provided equal velocities and foil thicknesses.

3.5 Electric-Field Stripping of H^0, H^- and H_2^+

Excited $H^*(n)$ atoms can be stripped at relatively low magnetic fields B, i.e., for $n > 3$, B = 0.5 T that corresponds to an electric field of 0.9 MV/cm, Table 6. The behavior of excited

Table 5: Calculated dissociative lifetimes of electronically excited states of H_2^+ ions. From [44]

State	D, eV	R_e, a_0	$\tau, 10^{-14}$ s
$1s\sigma_g$	2.7	2	
$2p\sigma_u$	0.0015	12.0	3.4
$2p\pi_u$	0.26	8.0	4.4
$3d\sigma_g$	1.4	9.0	3.0
$4d\sigma_g$	0.089	18.0	3.2
$4f\pi_u$	0.42	18.0	3.2
$4f\sigma_u$	0.15	20.0	
$5f\pi_g$	0.028	28.0	

Table 6: Critical electric field, $F = 5.7\times10^8/n^4$ V/cm, and corresponding magnetic B field (E = 800 MeV/u, $\beta = 0.84$) for ionization of hydrogen atoms in the n-state

n	F, V/cm	B(T)	n	F, V/cm	B(T)
1	5.7×10^8	121	6	4.4×10^5	0.093
2	3.6×10^7	7.6	7	2.4×10^5	0.050
3	7.0×10^6	1.5	8	1.4×10^5	0.030
4	2.2×10^6	0.47	9	8.7×10^4	0.018
5	9.1×10^5	0.19	10	5.7×10^4	0.012

$H^*(n)$ atoms in a magnetic (or in an electric field in the rest frame of the atom) is well understood and can be described by different approaches (see, for example, [34, 35, 36]). The one which is the most often used is the 5th-order perturbation theory developed by *Damburg* and *Kololsov* [34, 35].

The survival of the high-enery ions in accelerators is an important problem related with the static electric field induced in the ion's center of mass by the magnetic field used in the ion optics. In H^- ion, a loosely bound $1s$-electron with the binding energy $I = 0.754$ eV can be stripped by static fields of about 6×10^6 V/cm [48]. This electric field is close to ionize neutral hydrogen H(n) from the states between $n = 3$ and 4 (Table 6). The H_2^+ ions are supposed to be much more stable to electric fields (about two orders of magnitude) as compared to H^- because of the higher distruction energy (2.7 eV). Field-ionization of H^- ions was considered theoretically elsewhere (see, e.g. [49, 50]). It was found [50] that the H_2^+ ions can be stable up to electric fields of about 2×10^8 V/cm which is still small to ionize H atoms in the ground state. The results of comparison are presented in Table 7.

Table 7: Comparison of characteristics of H^- and H_2^+ Ion Beams

Characteristic	H^-	H_2^+
Ionization energy	0.75 eV	31.67 eV ($H^+ + H^+ + e$)
Dissociation energy	-	18.08 eV ($H^+ + H(1s)$)
		2.7 eV (depth of $1s\sigma_g$ state)
Production rate in ion source	low	high
Stripping electric field	6×10^6 V/cm	2×10^8 V/cm
Stripping magnetic field	1.28 kG	425 kG
Fraction of H^0	0.05	0.10 (estimated)
(E = 800 MeV/u, $x = 250$ μg/cm^2		
Source current	35 mA (70 mA required)	140 mA
Intensity	1.25×10^{13} proton/cycle	

Electronic band structure of H_2^+ for parallel internuclear and external magnetic field axes is considered in [37].

4 Conclusion

We have considered the ion-foil collision processes in relation with both fundamental elementary processes occuring in foils (loss, electron capture, excitation, dissociation etc.) and with application to the accelarator problems such as injection of protons formed by

stripping of relativistic H_2^+ and H^- ions in thin foils. In general, ion-foil collisions belong to unique domain of interactions because to understand and to describe the properties of these interactions, one has to apply principles of atomic, molecular and solid state physics simultaneously.

The problem of using relativistic H_2^+ molecular ions instead of H^- ions for spallation-neutron sources was reconsidered again. Because of higher ion production rate and higher stability against ionization by induced electric field, H_2^+ ions seem to be more perspective to be used in the future as compared to H^- ion beams. A fraction of neutral hydrogen created after H_2^+ ions passing through the foil, is estimated to be 2 times higher than for H^- ions because H_2^+ ions are more complicated atomic systems and therefore, more possible channels can contribute to formation of neutral hydrogen atoms which constitute the main beam losses. However, this circumstance does not destroy the general picture of advantages for using H_2^+ ions. Certainly, to obtain a more quantitative estimate, one has to carry out the corresponding experiments at relativistic energies or to perform sophisticated calculations on the basis of the advanced theories as, for example, the relativistic quantum stochastic approach as was discussed in Sect.3.1.

Aknowledgements. The authors are very grateful to I. Hofmann, R. Macek, R. Mann, H. Tawara and D. Zajfman for valuable remarks.

References

[1] R.J. Macek and the extended PSR Development Team: *Machine Studies at the Los Alamos Proton Storage Ring* In ICANS Twelve, Vol. 2, Rutherford Appleton Laboratory Report No. 94-025

[2] CERN Accelerator School (CAS), *Fifth General Accelerator Physics Course*, ed. S. Turner, Proceedings, Vol.II (Geneva 1994)

[3] I.S.K. Gardner, H. Lengeler, G.H. Rees (eds.): *Outline Design of the European Spallation Neutron Source*, Report ESS 95-30-M, European Spallation Source, September 1995

[4] E. Wilson: *Transverse Beam Dynamics* In *CERN Accelerator School (CAS), General Accelerator Physics*, eds. P. Bryant, S. Turner, 3 - 14 September 1984, Gif-sur-Yvette, Paris, France (Geneva 1985), Vol.1, p.65

[5] M.J. Gaillard, J.-C. Poizat, A. Ratkowski, J. Remillieux: Nucl. Instrum. Methods **132**, 69 (1976)

[6] Z. Chateau-Thierry, A. Gladieux, B. Delaunay: Nucl. Instrum. Methods **132**, 553 (1976)

[7] A.K. Eswards, R.M. Wood, M.F. Stauer: Phys. Rev. A **15**, 48 (1977)

[8] M.J. Gaillard, J.-C. Poizat, A. Ratkowski, J. Remillieux, M. Auzas: Phys. Rev. A **16**, 2323 (1977)

[9] N. Cue, N.V. de Castro-Faria, M.J. Gaillard, J.-C. Poizat, J. Remillieux: Nucl. Instrum. Methods **170**, 67 (1980)

[10] D.P. Almeida, N.V. de Castro Faria, F.L. Freire, Jr., E.C. Montenegro, A.G. de Pinho: Phys. Rev. A **36**, 16 (1987)

[11] Y. Yamazaki, N. Stolterfoht, P.D. Miller, H.F. Krause, P.L. Pepmiller, S. Datz, I.A. Sellin, J.N. Scheurer, S. Andriamonje, D. Bertault, J.F. Chemin: Phys. Rev. A **26**, 2913 (1988)

[12] D. Zajfman, G. Both, E.P. Kanter, Z. Vager: Phys. Rev. A **41**, 2482 (1990)

[13] D. Zajfman: Phys. Rev. A **42**, 5374 (1990)

[14] W. Brandt, R. Sizmann: In *Atomic Collisions in Solids*, Vol. 1 (Plenum, New York 1975)

[15] W. Brandt, R. Ritchie: Nucl. Instrum. Methods **132**, 43 (1976)

[16] M.C. Cross: Phys. Rev. B **15**, 602 (1977)

[17] N. Cue, N.V. de Castro-Faria, M.J. Gaillard, J.-C. Poizat, J. Remillieux, D.S. Gemmel, I. Plesser: Phys. Rev. Lett. **45**, 613 (1980)

[18] L.H. Toburen, M.Y. Nakai, R.A. Langley: Phys. Rev. **171**, 114 (1968)

[19] N. Bohr, K.Dann, Vidensk. Selsk. Mat. Fys. Medd. **18**, 105 (1948)

[20] R.K. Janev, L.P. Presnyakov, V.P. Shevelko: *Physics of Highly Charged Ions*, (Springer, Berlin-Heidelberg 1985)

[21] A.V. Vinogradov, A.M. Urnov, V.P. Shevelko: Sov. Phys. - JETP, **33**, 1110 (1971)

[22] H.H. Bukow, H. von Buttlar, D. Haas, P.H. Heckmann, M. Holl, W. Schlagheck, D. Schürmann, R. Tielert, R. Woodruff: Nucl. Instrum. Meth. **110**, 89 (1973)

[23] J. Remillieux: Nucl. Instrum. Meth. **170**, 31 (1980)

[24] E.P. Kanter, D. Schneider, Z. Vager: Phys. Rev. A **28**, 1193 (1983)

[25] K. Dybdal, J. Sørensen, P. Hvelplund, H. Knudsen: Nucl. Instrum. Meth. B **13**, 581 (1986)

[26] N. Cue, N.V. de Castro-Faria, M.J. Gaillard, J.-C. Poizat, J. Remillieux: Phys. Lett. A **72**, 104 (1979)

[27] M.M. Jakas, N.E. Capij: Nucl. Instrum. Meth. B **93**, 14 (1994)

[28] R. McCarroll, R.D. Piacentini, A.Salin: J. Phys. B **3**, 137 (1970)

[29] J. Davidson: Phys. Rev. A **12**, 1350 (1975)

[30] C.J. Anderson et. al.: Phys. Rev. A **22**, 822 (1980)

[31] T. Aberg, O. Goscincki: Phys. Rev. A **24**, 801 (1982)

[32] M.S. Gulley, P.B. Keating, H.C. Bryant, E.P. MacKerrow, W.A. Miller, D.C. Rislove, C. Cohen, J.B. Donahue, D.H. Fitzgerald, S.C. Frankle, D.J. Funk, R.L. Hutson, R.J. Macek, M.A. Plum, N.G. Stanciu, O.B. van Dyck, C.A. Wilkinson, C.W. Planner: Phys. Rev. A **53**, 3201 (1996)

[33] B. Gervais, C.O. Reinhold, J. Burgdörfer: Phys. Rev. A **53**, 3189 (1996)

[34] R.J. Damburg, V.V. Kolosov: J. Phys. B **9**, 3149 (1976)

[35] R.J. Damburg, V.V. Kolosov: In *Rydberg States of Atoms and Molecules*, ed. F. Stebbings (Cambridge University Press, 1983), pp.31 - 71

[36] F.M. Fernández: Phys. Rev. A **54**, 1206 (1996)

[37] U. Kappes, P. Schmelcher: Phys. Rev. A **51**, 4542 (1995)

[38] A.H. Mohagheghi, H.C. Bryant, P.G. Harris, R.A. Reeder, H. Sharifian, C.Y. Tang, H. Tootoonchi, C.R. Quick, S. Cohen, W.W. Smith, J.E. Srewart: Phys. Rev. A **43**, 1345 (1991)

[39] B. Gervais, J. Burgsdórfer: Nucl. Instrum. Methods **99**, 101 (1995)

[40] J. Burgdorfer, Ch. Bottcher: Phys. Rev. Lett. **61**, 2917 (1988)

[41] E.J. Galvez et al.: Phys. Rev Lett. **61**, 2011 (1988)

[42] Q. Su et al.: Phys. Rev Lett. **64**, 862 (1990)

[43] M. Font: Phys. Rev A **40**, 5659 (1990)

[44] E.A. Andreev, D. Böhne, V.L. Bychkov, V.P. Shevelko: Physica Scripta (1997), to be submitted

[45] R.J. Hutson: Los Alamos National Laboratory Report No. PSR-92-015 (1992)

[46] R.J. Macek: In *Proc. XIIth Meeting Intl. Collaboration on Adv. Neutral Sources*, Abingdon, Oxfordshire, 1993, ed. by U. Steigenberger et al., (science and Engineering Research Concil, Rutherford Appleton Lab., Chilton, 1993), Vol.II, pp. A25 - A32

[47] E.S. Chang: Phys. Rev. A **31**, 465 (1985)

[48] P.B. Keating, M.S. Gulley, H.C. Bryant et al.: Phys. Rev. A (1996, submitted for publication)

[49] J.R. Hiskes: Phys. Rev. **122**, 1207 (1961)

[50] J.M. Peek:*Dissociation of the Bound Vibration States of* H_2^+ *by a Uniform Electric Field*, Los Alamos National Laboratory Report (1996, to be published)

UNITS RELATIONS

Relativistic factors:

$$\beta = v/c = \sqrt{1 - \frac{1}{(1 + E/m_0c^2)^2}}, \tag{25}$$

where E is the energy of the projectile, m_0c^2 = 931.5 MeV for heavy particles, and m_0c^2 = 511 keV for electrons; the γ-factor is defined by

$$\gamma = 1 + \frac{E}{mc_0^2} = \frac{1}{\sqrt{1 - \beta^2}}. \tag{26}$$

Electric field strength F created in the rest frame of a particle moving with velocity v in the magnetic field B_{lab} is giben by (Lorentz force):

$$F[V/cm] = \gamma\beta c B_{lab}[T], \tag{27}$$

where T is a Tesla unit. For β = 0.84, 1T corresponds to 4.7 MV/cm.

1 a.u. of the field strength $F_0 = 5.142 \times 10^9$ V/cm.

1 T corresponds to 10^4 G (Gauss).

1 μg/cm$^2 \approx$ 50Å= 95 a.u.